Measurement of the product branching fraction $\mathcal{B}(c\to\Theta_c X)\times\mathcal{B}(\Theta_c\to\Lambda X)$

R. Ammar, P. Baringer, P. Brabant, A. Bean, D. Besson, H. Bull, R. Davis, J. Holliday, S. Kotov, I. Kravchenko, N. Kwak, I. Robertson, R. Stutz, and X. Zhao
University of Kansas, Lawrence, Kansas 66045

S. Anderson, V. V. Frolov, Y. Kubota, S. J. Lee, R. Mahapatra, J. J. O'Neill, R. Poling, T. Riehle, and A. Smith
University of Minnesota, Minneapolis, Minnesota 55455

S. Ahmed, M. S. Alam, S. B. Athar, L. Jian, L. Ling, A. H. Mahmood,* M. Saleem, S. Timm, and F. Wappler
State University of New York at Albany, Albany, New York 12222

A. Anastassov, J. E. Duboscq, K. K. Gan, C. Gwon, T. Hart, K. Honscheid, H. Kagan, R. Kass, J. Lorenc, H. Schwarthoff, E. von Toerne, and M. M. Zoeller
Ohio State University, Columbus, Ohio 43210

S. J. Richichi, H. Severini, P. Skubic, and A. Undrus
University of Oklahoma, Norman, Oklahoma 73019

M. Bishai, S. Chen, J. Fast, J. W. Hinson, J. Lee, N. Menon, D. H. Miller, E. I. Shibata, and I. P. J. Shipsey
Purdue University, West Lafayette, Indiana 47907

Y. Kwon,† A. L. Lyon, and E. H. Thorndike
University of Rochester, Rochester, New York 14627

C. P. Jessop, K. Lingel, H. Marsiske, M. L. Perl, V. Savinov, D. Ugolini, and X. Zhou
Stanford Linear Accelerator Center, Stanford University, Stanford, California 94309

T. E. Coan, V. Fadeyev, I. Korolkov, Y. Maravin, I. Narsky, R. Stroynowski, J. Ye, and T. Wlodek
Southern Methodist University, Dallas, Texas 75275

M. Artuso, R. Ayad, E. Dambasuren, S. Kopp, G. Majumder, G. C. Moneti, R. Mountain, S. Schuh, T. Skwarnicki, S. Stone, A. Titov, G. Viehhauser, J. C. Wang, A. Wolf, and J. Wu
Syracuse University, Syracuse, New York 13244

S. E. Csorna, K. W. McLean, S. Marka, and Z. Xu
Vanderbilt University, Nashville, Tennessee 37235

R. Godang, K. Kinoshita,‡ I. C. Lai, P. Pomianowski, and S. Schrenk
Virginia Polytechnic Institute and State University, Blacksburg, Virginia 24061

G. Bonvicini, D. Cinabro, R. Greene, L. P. Perera, and G. J. Zhou
Wayne State University, Detroit, Michigan 48202

S. Chan, G. Eigen, E. Lipeles, M. Schmidtler, A. Shapiro, W. M. Sun, J. Urheim, A. J. Weinstein, and F. Würthwein
California Institute of Technology, Pasadena, California 91125

D. E. Jaffe, G. Masek, H. P. Paar, E. M. Potter, S. Prell, and V. Sharma
University of California, San Diego, La Jolla, California 92093

D. M. Asner, A. Eppich, J. Gronberg, T. S. Hill, D. J. Lange, R. J. Morrison, T. K. Nelson, and J. D. Richman
University of California, Santa Barbara, California 93106

R. A. Briere
Carnegie Mellon University, Pittsburgh, Pennsylvania 15213

B. H. Behrens, W. T. Ford, A. Gritsan, H. Krieg, J. Roy, and J. G. Smith
University of Colorado, Boulder, Colorado 80309-0390

J. P. Alexander, R. Baker, C. Bebek, B. E. Berger, K. Berkelman, F. Blanc, V. Boisvert, D. G. Cassel, M. Dickson,

P. S. Drell, K. M. Ecklund, R. Ehrlich, A. D. Foland, P. Gaidarev, L. Gibbons, B. Gittelman, S. W. Gray, D. L. Hartill, B. K. Heltsley, P. I. Hopman, C. D. Jones, D. L. Kreinick, T. Lee, Y. Liu, T. O. Meyer, N. B. Mistry, C. R. Ng, E. Nordberg, J. R. Patterson, D. Peterson, D. Riley, J. G. Thayer, P. G. Thies, B. Valant-Spaight, and A. Warburton
Cornell University, Ithaca, New York 14853

P. Avery, M. Lohner, C. Prescott, A. I. Rubiera, J. Yelton, and J. Zheng
University of Florida, Gainesville, Florida 32611

G. Brandenburg, A. Ershov, Y. S. Gao, D. Y.-J. Kim, and R. Wilson
Harvard University, Cambridge, Massachusetts 02138

T. E. Browder, Y. Li, J. L. Rodriguez, and H. Yamamoto
University of Hawaii at Manoa, Honolulu, Hawaii 96822

T. Bergfeld, B. I. Eisenstein, J. Ernst, G. E. Gladding, G. D. Gollin, R. M. Hans, E. Johnson, I. Karliner, M. A. Marsh, M. Palmer, C. Plager, C. Sedlack, M. Selen, J. J. Thaler, and J. Williams
University of Illinois, Urbana-Champaign, Illinois 61801

K. W. Edwards
Carleton University, Ottawa, Ontario, Canada K1S 5B6
and the Institute of Particle Physics, Canada

R. Janicek and P. M. Patel
McGill University, Montréal, Québec, Canada H3A 2T8
and the Institute of Particle Physics, Canada

A. J. Sadoff
Ithaca College, Ithaca, New York 14850

(CLEO Collaboration)
(Received 28 April 2000; published 12 October 2000)

Based on a high statistics $e^+e^-\to c\bar{c}$ data sample, we report on the inclusive rate for charmed baryons to decay into Λ particles using charm-event tagging. We select $e^+e^-\to c\bar{c}$ events which have a clear anti-charm tag and measure the Λ content in the hemisphere opposite the tag (charge conjugate modes are implicit). This allows us to determine the product branching fraction $\mathcal{B}_\Lambda=\mathcal{B}(c\to\Theta_c X)\times\mathcal{B}(\Theta_c\to\Lambda X)$, where Θ_c represents a sum over all charmed baryons produced in e^+e^- fragmentation at $\sqrt{s}=10.5$ GeV, given our specific tags. We obtain $\mathcal{B}_\Lambda=(1.87\pm0.03\pm0.33)\%$.

PACS number(s): 13.30.−a, 13.60.Rj, 13.65.+i, 14.20.Lq

I. INTRODUCTION

Inclusive measurements of charmed baryon decay products provide essential information on the relative contributions of different decay processes (e.g., external W emission, internal W emission, W exchange) to the weak $c\to sW^+$ transition in baryons. Difficulties in distinguishing direct charm decay products from jet fragmentation particles have hampered such inclusive measurements. An example is the measurement of $\mathcal{B}(\Lambda_c\to\Lambda X)$ (although ''Λ_c'' here designates Λ_c^+, charge conjugation is implicit throughout). Using the total Λ yield at $\sqrt{s}=10$ GeV/c to measure $\mathcal{B}(\Lambda_c\to\Lambda X)$ requires separating the background Λ component due to light quark fragmentation from production via $c\to\Lambda_c\to\Lambda X$. The difficulty of separating fragmentation Λ's from those resulting from Λ_c decays can be overcome by using a tagged sample of $e^+e^-\to c\bar{c}$ events. In this analysis, we use charm-event tagging to measure the product of the likelihood for a charm quark to materialize as a charmed baryon Θ_c times the branching fraction for a charmed baryon to decay into a Λ: $\mathcal{B}(c\to\Theta_c X)\times\mathcal{B}(\Theta_c\to\Lambda X)$. From JETSET 7.3 Monte Carlo simulations [1], using the default LEP-tuned control parameters, we expect that ~88% of Θ_c particles produced in $e^+e^-\to c\bar{c}$ fragmentation at $\sqrt{s}=10$ GeV will be Λ_c's.

Previous measurements of $\mathcal{B}(\Lambda_c\to\Lambda X)$ have either measured the Λ production rate from data taken just above the $e^+e^-\to\Lambda_c\bar{\Lambda}_c$ threshold [2], from topologically tagged Λ_c decays [3], or derived a value for $\mathcal{B}(\Lambda_c\to\Lambda X)$ based on

*Permanent address: University of Texas - Pan American, Edinburg, TX 78539.
†Permanent address: Yonsei University, Seoul 120-749, Korea.
‡Permanent address: University of Cincinnati, Cincinnati, OH 45221.

measurements of baryon production in B-meson decay [4]. Knowing, for example, that $\mathcal{B}(B\to p/\bar{p}(\text{direct})+\text{anything}) = 5.5\pm 0.5\%$[5], $\mathcal{B}(B\to\Lambda/\bar{\Lambda}+\text{anything}) = 4.0\pm 0.5\%$, and assuming that $\bar{B}\to\Lambda_c\bar{N}\text{X}$ dominates baryon production in B decay, with $\bar{N}$ equally likely to be $\bar{p}$ or $\bar{n}$, one can estimate $\mathcal{B}(\Lambda_c\to\Lambda X)\sim 4/(5.5\times 2)=36\%$. This simpleminded estimate, however, needs to be modified to take into account many corrections, among them the recent result that $\mathcal{B}(\bar{B}\to\bar{\Lambda}X)/\mathcal{B}(\bar{B}\to\Lambda X)=0.43\pm 0.09\pm 0.07$ [6]. That latter result implies that only $\sim 2/3$ of the inclusive $(\Lambda+\bar{\Lambda})$ yield in $\bar{B}$ decay come from decays of charmed baryons; the remainder is presumably due to associated production or decay of anticharm baryons. In this article, we use a new technique to determine the product of the probability for a charm quark to produce a charmed baryon Θ_c times the probability that the charmed baryon will decay into a Λ: $\mathcal{B}_\Lambda=\mathcal{B}(c\to\Theta_c X)\times\mathcal{B}(\Theta_c\to\Lambda X)$, using continuum e^+e^- annihiliation events at $\sqrt{s}=10.55$ GeV.

A sample $c\bar{c}$ event is schematically shown below, showing some of the particles relevant to our measurement. In that event, the fragmentation of the original $c\bar{c}$ quark-antiquark results in a Λ recoiling in one hemisphere opposite the anticharm tag (either the soft pion or the electron) in the other hemisphere. For this analysis, event ''hemispheres'' are defined using the axis which minimizes the momentum (charged plus neutral) transverse to that axis (the ''thrust'' axis). Note that both the soft pion and the electron are of charge opposite to the p daughter of the Λ. In addition to the tags depicted below, we also tag $c\bar{c}$ events with fully reconstructed $\bar{D}^0\to K^+\pi^-$ or $D^-\to K^+\pi^-\pi^-$ events, in which the $\bar{D}$ daughter kaon contains an $\bar{s}$ quark, in contrast to the Λ. For all four tags, we will therefore refer to our signal as an opposite hemisphere, opposite sign (OH-OS) correlation:

$$
\begin{array}{ccccc}
 & & c & \bar{c} & \\
 & \Lambda_c\hookleftarrow & & \hookrightarrow D^{*-} & \\
\Lambda X\hookleftarrow & & & & \hookrightarrow \pi^-_{soft}+\bar{D}^0 \\
p+\pi^-\hookleftarrow & & & & \hookrightarrow e^-+\bar{\nu}_e+K^+.
\end{array}
$$

We note that the Λ_c in this example can, in practice, be any charmed baryon and will from here on be denoted as ''Θ_c.''

II. APPARATUS AND EVENT SELECTION

This analysis was performed using the CLEO II detector operating at the Cornell Electron Storage Ring (CESR) at center-of-mass energies $\sqrt{s}=10.52$–10.58 GeV. The CLEO II detector is a general purpose solenoidal magnet spectrometer and calorimeter designed to trigger efficiently on two-photon, tau-pair, and hadronic events [7]. Measurements of charged particle momenta are made with three nested coaxial drift chambers consisting of 6, 10, and 51 layers, respectively. These chambers fill the volume from $r=3$ cm to $r=1$ m, with r the radial coordinate relative to the beam ($\hat{z}$) axis. This system is very efficient ($\epsilon\geqslant 98\%$) for detecting tracks that have transverse momenta (p_T) relative to the beam axis greater than 200 MeV/c and that are contained within the good fiducial volume of the drift chamber ($|\cos\theta|<0.94$, with θ defined as the polar angle relative to the beam axis). This system achieves a momentum resolution of $(\delta p/p)^2=(0.0015p)^2+(0.005)^2$ (p is the momentum, measured in GeV/c). Pulse height measurements in the main drift chamber provide specific ionization resolution of 5.5% for Bhabha events, giving good K/π separation for tracks with momenta up to 700 MeV/c and separation of the order of 2σ in the relativistic rise region above 2 GeV/c. Outside the central tracking chambers are plastic scintillation counters, which are used as a fast element in the trigger system and also provide particle identification information from time of flight measurements.

Beyond the time-of-flight system is the electromagnetic calorimeter, consisting of 7800 thallium-doped CsI crystals. The central ''barrel'' region of the calorimeter covers about 75% of the solid angle and has an energy resolution which is empirically found to follow:

$$\frac{\sigma_E}{E}(\%)=\frac{0.35}{E^{0.75}}+1.9-0.1E; \qquad (1)$$

E is the shower energy in GeV. This parametrization includes effects such as noise, and translates to an energy resolution of about 4% at 100 MeV and 1.2% at 5 GeV. Two end-cap regions of the crystal calorimeter extend solid angle coverage to about 95% of 4π, although energy resolution is not as good as that of the barrel region. The tracking system, time of flight counters, and calorimeter are all contained within a superconducting coil operated at 1.5 T. Flux return and tracking chambers used for muon detection are located immediately outside the coil and in the two end-cap regions.

For all four tags, data used for this measurement includes 3.1 fb^{-1} of data collected at the $\Upsilon(4S)$ resonance and 1.6 fb^{-1} of data collected about 60 MeV below the $\Upsilon(4S)$ resonance. This sample is augmented for the lower-efficiency $\bar{D}$ tags, as described later. For our analysis, we select continuum hadronic events which contain either a low-

momentum pion π^-_{soft} emitted at small angles relative to the event thrust axis (from $D^{*-}\to\bar{D}^0\pi^-_{soft}$), a high momentum electron (from $\bar{c}\to\bar{s}e^-\nu_e$), or a fully reconstructed $\bar{D}^0\to K^+\pi^-$ or $D^-\to K^+\pi^-\pi^-$ as a tag of $e^+e^-\to c\bar{c}$ events. In order to suppress background and enrich the hadronic fraction of our event sample, we impose several event requirements. Candidate events must have (1) at least five detected, good quality, charged tracks, (2) an event vertex consistent with the known e^+e^- interaction point, and (3) a total measured visible event energy, equal to the sum of the observed charged plus neutral energy E_{vis} $(=E_{chrg}+E_{neutral})$, greater than 110% of the single beam energy, $E_{vis}>1.1E_{beam}$. In addition, when using an electron to tag a $c\bar{c}$ event we require that either the beam energy E_{beam} be less than 5.275 GeV or that the event be well collimated. Specifically, the ratio of Fox-Wolfram event shape parameters $H2/H0$ can be used to quantify the ''jettiness'' of an event [8]. For a perfectly spherical flow of event energy, this ratio equals 0; for a perfectly jetty event, this ratio equals 1.0. For our electron tags, we require this ratio to be greater than 0.35. This requirement is necessary to remove contamination from $B\bar{B}$ events. Similarly, when using $\bar{D}^0\to K^+\pi^-$ or $D^-\to K^+\pi^-\pi^-$ as our charm tags, we eliminate $B\bar{B}$ background by requiring that the reconstructed $\bar{D}$ momentum exceed 2.3 GeV/c.

III. TAG IDENTIFICATION

A. Electron tags

To suppress background from fake electrons, as well as true electrons not necessarily associated with $e^+e^-\to c\bar{c}$ events, we require that our electron-tag candidates satisfy the following criteria:

(a) The electron must pass a strict ''probability of electron'' identification criterion. This identification likelihood combines measurements of a given track's specific ionization deposition in the central drift chamber with the ratio of the energy of the associated calorimeter shower to the charged track's momentum [9]. True electrons have shower energies approximately equal to their drift chamber momenta; hadrons tend to be minimum ionizing and have considerably smaller values of shower energy relative to their measured momenta. We require that the natural logarithm of the ratio of a charged track's electron probability relative to the probability that the charged track is a hadron L_e be greater than 7 $(\mathsf{L}_e\geqslant 7)$.

(b) The momentum of the electron must be greater than 1 GeV/c. This criterion helps eliminate kaon and pion fakes and also suppresses electrons from photon conversions ($\gamma\to e^+e^-$) and π^0 Dalitz decays ($\pi^0\to\gamma e^+e^-$).

(c) The electron must have an impact parameter relative to the event vertex less than 4 mm along the radial coordinate and no more than 2 cm along the beam axis. This provides additional suppression of electrons resulting from photon conversions.

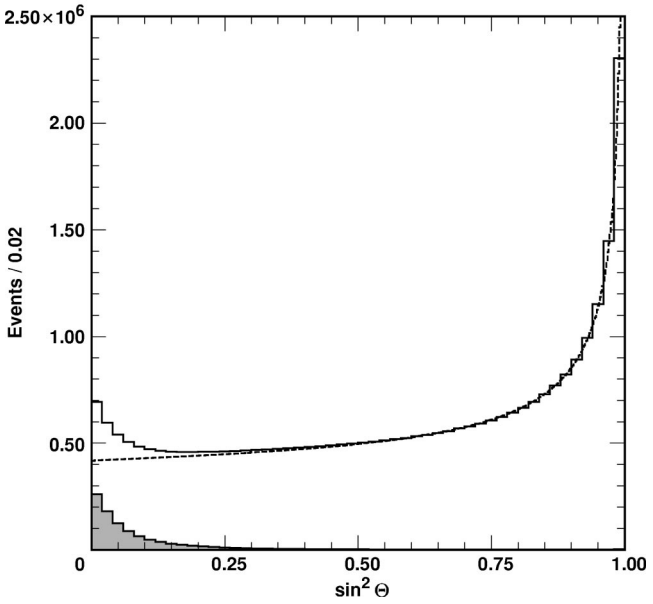

FIG. 1. $\sin^2\theta$ distribution for candidate π^-_{soft}. Shown is the inclusive distribution (solid histogram) overlaid with the background fit function (dashed line) and the signal expected from D^{*-} decays (shaded).

B. Soft pion tags

Our soft pion tag candidates must pass the following restrictions:

(a) The pion must have an impact parameter relative to the event vertex less than 5 mm along the radial coordinate and no more than 5 cm along the beam axis.

(b) The pion must pass a 99% probability criterion for pion identification, based on the associated charged track's specific ionization measured in the drift chamber.

(c) The pion's measured momentum must be between 0.15 GeV/c and 0.40 GeV/c.

(d) The pion's trajectory must lie near the trajectory of the parent charm quark, as expected for pions produced in $D^{*-}\to\bar{D}^0\pi^-_{soft}$. Experimentally, this is checked using the variable $\sin^2\theta$, with θ the opening angle between the candidate soft pion and the event thrust axis. Assuming that the thrust axis approximates the original $c\bar{c}$ axis, true π^-_{soft} should populate the region $\sin^2\theta\to 0$. Figure 1 displays the $\sin^2\theta$ distribution for candidates passing our event and track selection criteria. The excess in the region $\sin^2\theta$ near 0 constitutes our charm-tagged sample. The fit includes a signal contribution, the shape of which is determined from Monte Carlo simulations, and a lower-order polynomial to fit the background. The technique for determining the signal shape and background follows that of an earlier CLEO analysis [10], which used this method to measure the branching fraction $\mathcal{B}(D^0\to K^-\pi^+)$.

C. $\bar{D}^0\to K^+\pi^-$ and $D^-\to K^+\pi^-\pi^-$ tags

The $\bar{D}$-tagged analysis was performed independent of the π^-_{soft} and electron-tagged analyses. For this latter analysis, we take advantage of improved track and particle reconstruc-

tion algorithms, which were unavailable when the π^-_{soft} and electron-tagged analyses were conducted. Also, in order to compensate for the intrinsically smaller efficiency of $\overline{D}^0 \to K^+\pi^-$ and $D^- \to K^+\pi^-\pi^-$ reconstruction, we use a threefold larger data sample ($13.1\,\mathrm{fb}^{-1}$, including the CLEO II.V data set [11]) for this analysis. Note that, for the purpose of this analysis, which does not utilize the precision vertexing afforded by the CLEO II.V silicon vertex system, the essential detector performance characteristics are the same as for the CLEO II data sample. $\overline{D}^0 \to K^+\pi^-$ and $D^- \to K^+\pi^-\pi^-$ tags are fully reconstructed from kaon and pion candidates as follows:

(a) The kaon and pion candidates must have impact parameters relative to the event vertex less than 5 mm along the radial coordinate and no more than 5 cm along the beam axis.

(b) Both the pion and kaon tracks must be consistent with their assumed particle identities at the level of 2.5 standard deviations (σ), using the available specific ionization and time-of-flight particle identification information.

(c) Both the pion and kaon must have momentum greater than 0.3 GeV/c.

(d) The fully reconstructed $\overline{D}$ meson tag must have momentum greater than 2.3 GeV/c to eliminate $B\overline{B}$ backgrounds.

IV. LAMBDA DETECTION

After finding a charm tag, we reconstruct $\Lambda \to p\pi$ in the hemisphere opposite the tag. In addition to a 99% particle identification probability requirement placed on both the daughter proton and pion used in reconstructing the Λ, we also require that candidate Λ particles have momenta greater than 1 GeV/c and that the lambda vertex be located at least 2 cm away from the e^+e^- collision point in the radial direction. According to Monte Carlo simulations (Fig. 2), imposing the minimum Λ momentum requirement ($p_\Lambda > 1.0$ GeV) in a charm-tagged event passing our event selection requirements results in a Λ sample which is $>95\%$ pure $\Theta_c \to \Lambda X$, with the remaining Λ's due to light quark fragmentation.

V. YIELDS

To extract our signal yields in the lepton-tagged sample, we plot the proton-pion invariant mass for Λ candidates in electron-tagged events. Figure 3 shows the candidate Λ mass separated into each of the four possible sign-hemisphere correlations. Our candidate signal Λ's are contained in Fig. 3d (lower right). The number of signal Λ's is extracted by fitting a Gaussian Λ signal function plus a second-order Chebyschev polynomial background.

To determine the Λ yield in π^-_{soft} tagged events, we plot the $\sin^2\theta$ of the π-thrust axis angle for each candidate Λ found vs the candidate $p^+\pi^-$ mass. We then project the resulting histogram onto the $\sin^2\theta$ axis and fit the peak at $\sin^2\theta \to 0$ for the case where the $p^+\pi^-$ invariant mass is in the Λ region (signal) versus the case where the $p^+\pi^-$ invariant mass is in the Λ sidebands. After performing a sideband subtraction in Λ mass of the two $\sin^2\theta$ distributions, we obtain Fig. 4. A fit to the $\sin^2\theta$ distribution for all pion candidates (Fig. 1) determines our total number of π^-_{soft}-tagged $c\overline{c}$ events (the denominator in our ratio).

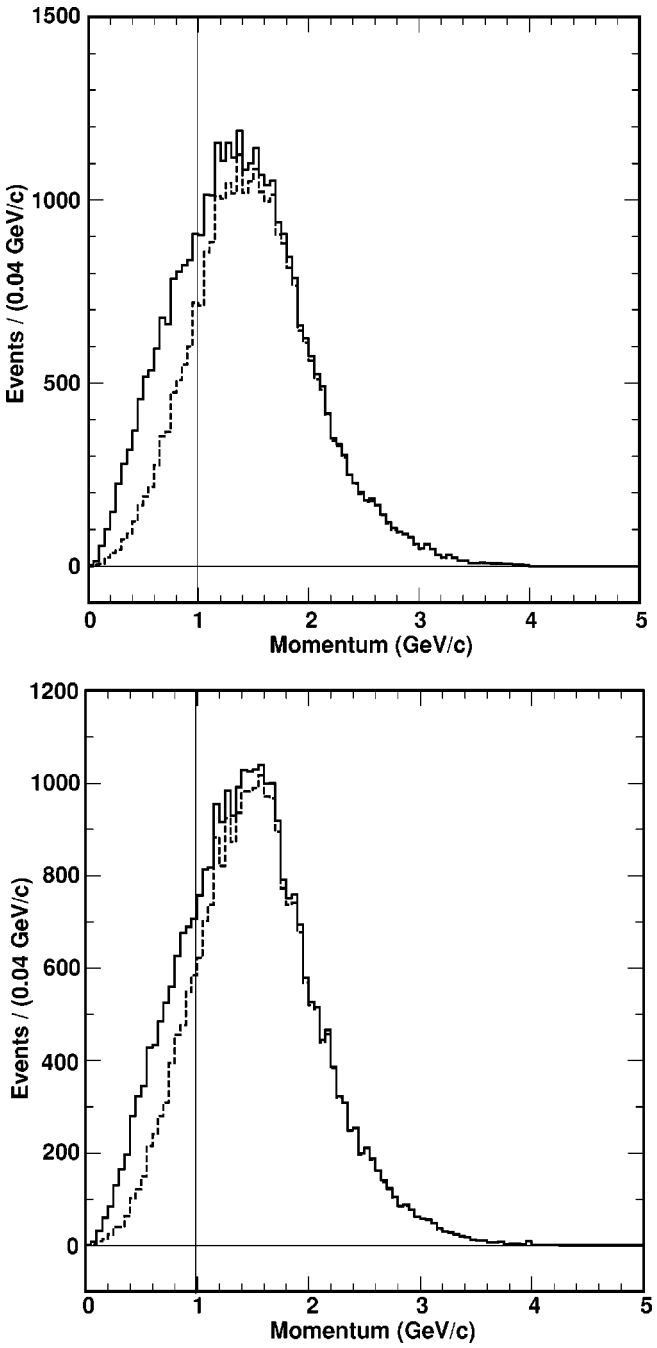

FIG. 2. JETSET 7.3 Monte Carlo simulations of momentum spectra for Λ's passing our tag, event, and opposite-hemisphere–opposite sign (OH-OS) requirements, for electron tags (left) and soft pion tags (right). Shown are all Λ's in $c\overline{c}$ events (solid) compared to Λ's which decay from charmed baryons (dashed). Our minimum momentum requirement ($p_\Lambda > 1$ GeV/c) is also indicated.

Monte Carlo simulations indicate that both (i) the fraction

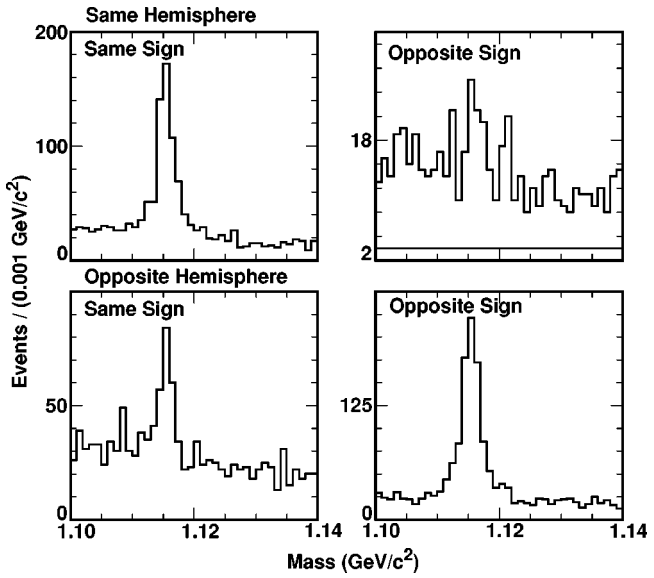

FIG. 3. Candidate Λ particles from data divided into same-opposite hemisphere-sign correlations using the electron tag. Opposite-hemisphere–opposite sign Λ's (lower right) result predominantly from $\Lambda_c \to \Lambda X$; Λ-electron correlations can be seen from processes such as $\Theta_c \to \Lambda e^- \nu_e X$ decays (same hemisphere, same sign), $\bar{c} \to \Lambda \bar{\Theta}_c$, $\bar{\Theta}_c \to e^- \nu_e X$ decays (same hemisphere, opposite sign) and $X e^- \nu_e \leftarrow \bar{c}c \to \Theta_c \bar{\Lambda}$ decays (opposite hemisphere, same sign). From the known electron fake rate, we conclude that fakes contribute from ~10–40 events to each of the Λ peaks. Since the hemisphere correlation is not rigorous, we also note that some of the ''wrong hemisphere'' correlation is due to leakage into the opposite hemisphere from real $\Theta_c \to \Lambda X$ or real semileptonic decays.

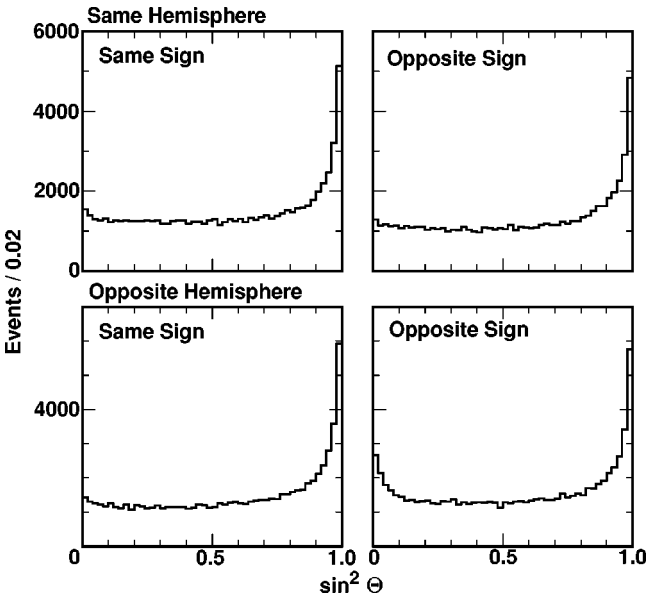

FIG. 4. Four possible Λ/π^-_{soft} correlations, after Λ sideband subtraction (as described in text).

of non-$c\bar{c}$ tags and (ii) the fraction of candidate signal Λ's that do not originate from Θ_c decays but pass our selection criteria are small ($<3\%$; see Fig. 2). We test the overall accuracy of the Monte Carlo by comparing same-sign, opposite hemisphere correlation events (''SS-OH,'' i.e. opposite of the sign correlation expected for signal) in simulations compared to data. We find that the ratio of SS-OH electron-Λ correlation events to the number of ''right sign'' (OS-OH) signal events is 0.19 ± 0.05 in Monte Carlo simulations and 0.19 ± 0.07 in data. The corresponding values for the $\pi^-_{soft} - \Lambda$ correlations are 0.09 and 0.16, respectively. Within statistics, the Monte Carlo reproduces the ''wrong sign'' (SS-OH) fractions observed in data. Nevertheless, we conservatively assign a relative systematic error of 10% (19%/2) to reflect our confidence in the simulations. This value is entered in the final systematic errors table (Table IV) as ''Event generator mismodeling.''

For the $\bar{D}$-tagged sample, the signal is extracted from a two-dimensional plot of M_Λ (the mass of the Λ candidate) vs $M_{\bar{D}}$ (the mass of the $\bar{D}$-tag candidate, either $M_{K^+\pi^-}$ or $M_{K^+\pi^-\pi^-}$), as indicated in Figs. 5 and 6. Our signal comprises events which contain both a fully reconstructed $\bar{D}$ and also a Λ (''double tags''). The double-tag signal yields are determined by a two-dimensional sideband subtraction technique, similar to that used to determine the signal yield for the soft-pion tagged sample. Here, we subtract the scaled Λ yield in the $\bar{D}$ sideband region from the Λ yield in the $\bar{D}$ signal region. The resulting excess, is, by definition, our double-tag signal. As a check of the signal extraction, the yield for the ''wrong-sign'' double-tag signal (i.e., $D^0 \to K^- \pi^+$ vs $D^0 \to K^- \pi^+$) is similarly extracted using the same subtraction. In such events, the expected true correlated signal should be negligible and non-zero only through doubly Cabibbo suppressed decays [12]; in fact, we find -15

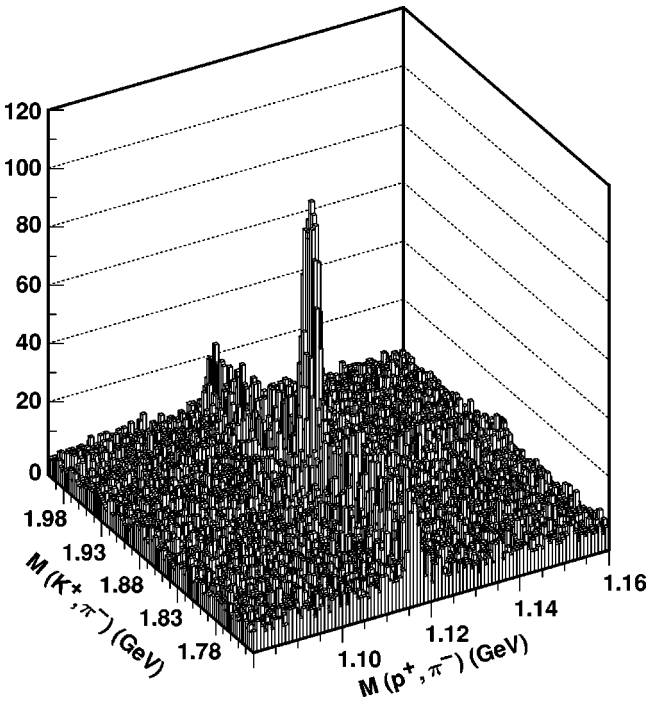

FIG. 5. Candidate $\bar{D}^0 \to K^+ \pi^-$ mass vs opposite hemisphere candidate $\Lambda \to p \pi^-$ mass.

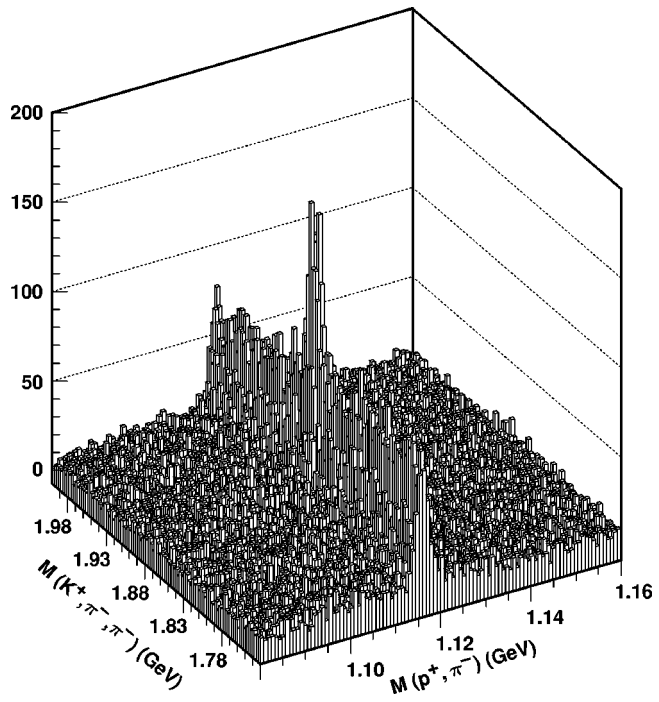

FIG. 6. Candidate $D^- \to K^+\pi^-\pi^-$ mass vs opposite hemisphere candidate $\Lambda \to p\pi^-$ mass.

± 25 events from a two-dimensional $M(K^-\pi^+)$ vs $M(K^-\pi^+)$ plot, and -115 ± 157 events from the two-dimensional $M(K^-\pi^+\pi^+)$ vs $M(K^-\pi^+\pi^+)$ plot. Note that the wrong-sign, wrong-hemisphere correlations are not only smaller in magnitude for the $\bar{D}$-tagged sample than the single-track tagged sample, but the agreement between the data and Monte Carlo simulation is generally better for the $\bar{D}$-tagged sample.

VI. CALCULATIONS

The product branching fraction $\mathcal{B}(c \to \Theta_c) \times \mathcal{B}(\Theta_c \to \Lambda X)$ can be derived from $N(\Lambda)/c\bar{c}$, the fraction of times that an event containing an anti-charm tag in one hemisphere contains a Λ in the opposite hemisphere. $N(\Lambda)/c\bar{c}$ should equal the probability of a c quark fragmenting to produce a Θ_c multiplied by the probability of the Θ_c to decay to a Λ multiplied by the efficiency for detection of a Λ in our charm-tagged event sample. Thus, in equation form, with $N(\Lambda)/c\bar{c}$ as the ratio of the number of reconstructed Λ's in tagged $c\bar{c}$ events to the total number of $c\bar{c}$ event tags, we have

$$\frac{N(\Lambda)}{c\bar{c}} = \mathcal{B}(c \to \Theta_c) \times \mathcal{B}(\Theta_c \to \Lambda X) \times \epsilon_{\Lambda, tagged} \qquad (2)$$

for both the data and Monte Carlo simulation. Assuming that the Monte Carlo simulation accurately reproduces the efficiency for finding a Λ in a tagged event ($\epsilon_{\Lambda,tagged}$ in this equation), the yield of non-$c\bar{c}$ tags ($<4\%$) and the fraction of non-signal Λ-tag correlations ($<5\%$), we can then calibrate our observed value of Λ's per $c\bar{c}$ in data to the Monte Carlo simulation:

$$\frac{\dfrac{N(\Lambda)^{data}}{c\bar{c}}}{\dfrac{N(\Lambda)^{MC}}{c\bar{c}}} = \frac{\mathcal{B}(c \to \Theta_c X) \times \mathcal{B}(\Theta_c \to \Lambda X)^{data}}{\mathcal{B}(c \to \Theta_c X) \times \mathcal{B}(\Theta_c \to \Lambda X)^{MC}}; \qquad (3)$$

the Monte Carlo values for $\mathcal{B}(c \to \Theta_c X)$ and $\mathcal{B}(\Theta_c \to \Lambda X)$ are 0.0667 and 0.369, respectively. [A recent measurement by the ALEPH Collaboration [14] at $\sqrt{s} = 90$ GeV has determined $\mathcal{B}(c \to \Lambda_c X) = 0.079 \pm 0.008 \pm 0.004 \pm 0.020$ (the last systematic error represents the uncertainty in the $\Lambda_c \to pK^-\pi^+$ branching fraction), although it is not clear how appropriate this value is for $\sqrt{s} = 10$ GeV.] Note that the efficiency $\epsilon_{\Lambda,tagged}$ is tag dependent—because of geometric and momentum correlations from hemisphere to hemisphere, we expect the highest efficiency for the $\bar{D}^0$ and D^- tags, followed by soft pion tags and electron tags.

A summary of our yields and calculations for $\mathcal{B}(c \to \Theta_c X) \times \mathcal{B}(\Theta_c \to \Lambda X)$ is presented in Tables I and II. Pre-

TABLE I. Results for $\mathcal{B}(c \to \Lambda_c) \times \mathcal{B}(\Lambda_c \to \Lambda X)$ using electrons, π^-_{soft}, and $\bar{D}$ to tag $c\bar{c}$ events.

Tag particle		Electron	π	$\bar{D}^0$	D^-
Total tags		177700 ± 422	1060870 ± 3942	325200 ± 1040	256730 ± 1180
Fake tags	$\gamma\gamma$	4665 ± 98			
	$\tau\tau$	9429 ± 97			
	$B\bar{B}$	15037 ± 123			
Total corrected tags		148569 ± 460	1060870 ± 3942	325200 ± 1040	256730 ± 1180
Λ's		743 ± 32	5964 ± 203	2247 ± 75	2031 ± 102
$\frac{N(\Lambda)}{c\bar{c}}$ $(\times 10^{-4})$		50 ± 2	56 ± 2	69 ± 2	79 ± 4
Monte Carlo $\frac{N(\Lambda)}{c\bar{c}}$ $(\times 10^{-4})$		76 ± 3	90 ± 2	80 ± 2	93 ± 4
Data B_Λ		0.0162 ± 0.0010	0.0153 ± 0.0006	0.0212 ± 0.0008	0.0209 ± 0.0013

TABLE II. Tabulated number of Λ's detected for both signal and non-signal correlations followed by $\Lambda/c\bar{c}$. For π^-_{soft} and e^-, a data sample corresponding to $\sim 5\times 10^6$ $c\bar{c}$ events was used; $\bar{D}^0$ and D^- tags are derived from a dataset of $\sim 15\times 10^6$ $c\bar{c}$ events. In both cases, the Monte Carlo simulated data sample is of comparable or slightly larger size. Shown are opposite hemisphere (OH), same hemisphere (SH), opposite sign (OS) and same sign (SS) correlations.

Correlation	Electron	π	$\bar{D}^0$	D^-
Data				
SH, SS	445±26	1039±170	252±33	220±34
SH, OS	43±13	484±186	14±24	12±38
OH, SS	142±19	914±356	223±76	233±91
OH, OS	743±32	5964±203	2247±75	2031±102
$\frac{\Lambda}{c\bar{c}}$ SH, SS ($\times 10^{-4}$)	32.3±1.9	9.8±1.6	7.8±1.0	8.6±1.3
$\frac{\Lambda}{c\bar{c}}$ SH, OS ($\times 10^{-4}$)	3.1±0.9	4.6±1.8	0.4±0.6	0.4±0.8
$\frac{\Lambda}{c\bar{c}}$ OH, SS ($\times 10^{-4}$)	10.3±1.4	9±3	7.2±2.3	9.1±3.6
$\frac{\Lambda}{c\bar{c}}$ OH, OS ($\times 10^{-4}$)	50±2	56±2	69±2	79±4
Monte Carlo				
SH, SS	573±29	5469±363	182±52	179±65
SH, OS	62±13	1448±381	44±23	4±46
OH, SS	264±24	2251±409	285±104	114±62
OH, OS	1352±61	26413±643	2073±65	1514±85
$\frac{\Lambda}{c\bar{c}}$ SH, SS ($\times 10^{-4}$)	32±2	19±2	7±2	11±4
$\frac{\Lambda}{c\bar{c}}$ SH, OS ($\times 10^{-4}$)	4±1	5±1	2±1	3±2
$\frac{\Lambda}{c\bar{c}}$ OH, SS ($\times 10^{-4}$)	15±2	8±2	11±5	7±4
Monte Carlo $\frac{\Lambda}{c\bar{c}}$ OH, OS ($\times 10^{-4}$)	76±3	90±2	80±2	93±4

sented in those tables are our raw yields, the number of true electrons which do not tag $c\bar{c}$ events (''fake tags''), and the number of Λ's reconstructed in the opposite hemisphere for our electron-tagged, soft pion-tagged, and $\bar{D}$-tagged samples. Backgrounds in the electron-tagged sample from $B\bar{B}$ and $\tau\bar{\tau}$ events are estimated from a large sample of Monte Carlo events, using a CLEO event generator for B decays and KORALB [13] for $\tau\bar{\tau}$ decays. The electron background from $\gamma\gamma$ events is estimated from the forward-backward excess of positrons versus electrons, compared to the expectation from QED. Our raw yields (prior to any scaling correction, described later) correspond to $\mathcal{B}_\Lambda=(1.62\pm 0.10)\%$ using electrons to tag $c\bar{c}$ events, $\mathcal{B}_\Lambda=(1.53\pm 0.06)\%$ using π^-_{soft} to tag $c\bar{c}$ events, $\mathcal{B}_\Lambda=(2.12\pm 0.08)\%$ using $\bar{D}^0$ to tag $c\bar{c}$ events, and $\mathcal{B}_\Lambda=(2.09\pm 0.13)\%$ using D^- to tag $c\bar{c}$ events (statistical errors only).

VII. CROSS-CHECKS

We have conducted two cross-checks to verify the accuracy of our derived result for $\mathcal{B}_\Lambda$. We emphasize that these are not measurements in themselves (and therefore have no

TABLE III. Results of analyzing the $\mathcal{B}(D^0 \to K^- \pi^+)$ cross-check.

Tag particle		Electron	π	$\bar{D}^0$	D^-
Total tags		177700±422	1060870±3942	325200±1040	256730±1180
Fake tags	$\gamma\gamma$	4665±68			
	$\tau\tau$	9429±97			
	$B\bar{B}$	15037±123			
Actual tags		148569±460	1060870±3942	325200±1040	256730±1180
D^0's		1154±41	10029±213	1965±61	1244±144
Data $\frac{N(D^0)}{c\bar{c}}$ ($\times 10^{-4}$)		78±3	94±2	121±4	123±9
Monte Carls $\frac{N(D^0)}{c\bar{c}}$ ($\times 10^{-4}$)		80±3	96±2	119±4	113±11
Scale factor		1.03±0.05	1.02±0.03	0.98±0.06	0.92±0.12

quoted systematic errors), but are presented only to verify our $\mathcal{B}_\Lambda$ measurement.

A. $D^0 \to K^- \pi^+$ decays

As a first cross-check, we compare the data- versus Monte Carlo simulation–derived values for the product branching fraction $\mathcal{B}(c \to D^0) \times \mathcal{B}(D^0 \to K^- \pi^+)$, using charm tagging. Since the branching fraction for $D^0 \to K^- \pi^+$ is known precisely, and since the fractional uncertainty in $\mathcal{B}(c \to D^0)$ is expected to be smaller than the corresponding uncertainty in $\mathcal{B}(c \to \Lambda_c)$, we can compare the value of $\mathcal{B}(c \to D^0) \times \mathcal{B}(D^0 \to K^- \pi^+)$ measured with charm tagging in data versus Monte Carlo simulations and thereby verify the method used in the Λ measurement. Using the same charm-tagged sample as before, we therefore search for the decay $D^0 \to K^- \pi^+$ (using the same requirements mentioned before) opposite the tag rather than $\Lambda \to p \pi^-$. As before, we perform a sideband subtraction to determine the number of $D^0 \to K^- \pi^+$ decays in our π^-_{soft} charm tagged sample. We thus use the same equation as with our Λ analysis, only modified for the $D^0 \to K^- \pi^+$ decay mode:

$$\frac{N(K^- \pi^+)}{c\bar{c}} = \mathcal{B}(c \to D^0) \times \mathcal{B}(D^0 \to K^- \pi^+) \times \epsilon_{D^0 \to K^- \pi^+}. \tag{4}$$

Again, assuming that the Monte Carlo accurately reproduces the efficiency for finding a D^0 decay in a tagged event, we calibrate our observed value of D^0's per $c\bar{c}$ in data to the Monte Carlo simulation:

$$\frac{\frac{N(K\pi)^{data}}{c\bar{c}}}{\frac{N(K\pi)^{MC}}{c\bar{c}}} = \frac{\mathcal{B}(c \to D^0) \times \mathcal{B}(D^0 \to K\pi)^{data}}{\mathcal{B}(c \to D^0) \times \mathcal{B}(D^0 \to K\pi)^{MC}}. \tag{5}$$

The results of our D^0 cross-check are presented in Table III. The Monte Carlo simulation adequately reproduces the $D^0 \to K^- \pi^+$ yield per $\bar{c}$ tag. Based on the consistency between these values and the known $D^0 \to K^- \pi^+$ branching fraction, a scale factor is applied to the data and a systematic error is added which reflects only the statistical precision of this cross-check. In all cases, the scale factor (Table III) is consistent with unity.

B. $\Lambda_c \to \Lambda e \nu_e$ decays

A second cross-check is afforded by our Λ-electron correlation sample. We note that the same-hemisphere, same-sign events are expected to be dominated by $\Lambda_c \to \Lambda e^+ \nu_e$ decays. Since the $\Lambda_c \to \Lambda e \nu_e$ branching fraction has been measured, we can use the relative ratio of the same-hemisphere, same-sign Λ-electron events, compared to the opposite-hemisphere, opposite-sign events to estimate the $\Lambda_c \to \Lambda X$ branching fraction. This estimate is ''internally normalizing''; i.e., we do not need to measure the fraction of our total charm tags which contain Λ's. We can relate the branching fractions $\mathcal{B}(\Lambda_c \to \Lambda e \nu_e)$ and $\mathcal{B}(\Lambda_c \to \Lambda X)$ (and their corresponding efficiencies ϵ) to the number of observed same-hemisphere, same-sign events ($N_{SH\text{-}SS}$), the number of observed opposite hemisphere, opposite sign events $N_{OH\text{-}OS}$, and their production fractions in $c\bar{c}$ events. Without an explicit fake electron subtraction to the observed yields, we have

TABLE IV. Summary of systematic errors for both electron, soft pion, $\overline{D}^0$ and D^--tagged events. Correlated systematic errors are indicated with an asterisk (*).

Systematic (Variation/Default)	e^-	π^-_{soft} Tag	$\overline{D}^0$	D^-
Event requirements				
Minimum event energy: 0.88–1.32E_{beam} (1.1E_{beam})	2%	3%	2%	2%
Minimum number of charged tracks: 3–7 (5)	7%	3%	2%	2%
Tag requirements				
Tag momentum: 0.8–1.2× default	8%	3%	4%	4%
Radially close to event vertex: 0.8–1.2× default	2%	3%		
Tag DOCA along beam axis: 4–6 cm (5 cm)	2%	3%		
Probability of being a pion: $2.4\sigma-3.6\sigma$ (3σ)		3%		
Minimum electron probability: $L_e \geq 7$ ($L_e \geq 5$)	9%			
Event sphericity cut: $0.25 \leq R2 \leq 0.45$ (0.35)	6%	—		
Signal extraction	5%	13%	8%	8%
Event generator mismodeling	10%	10%	5%	6%
Lambda requirements*				
Lambda momentum: 0.8–1.2 GeV/c (1.0 GeV/c)	6%	6%	6%	6%
Radial cut on Λ vertex: 1.6–2.4 cm (2.0 cm)	3%	3%	3%	3%
Additional systematics				
Tracking-finding uncertainty*	4%	4%	4%	4%
D0 cross-check	5%	3%	6%	14%
Total correlated systematic	8%	8%	8%	8%
Total uncorrelated systematic	19%	18%	11%	18%
RMS spread of tag values		14%		
Total systematic uncertainty	25%	24%	20%	24%

$$\frac{N_{SH\text{-}SS}}{N_{OH\text{-}OS}} \approx \frac{\mathcal{B}(c\to\Lambda_c)\times\mathcal{B}(\Lambda_c\to\Lambda e\nu_e)\times\epsilon(\Lambda_c\to\Lambda e\nu_e)}{\mathcal{B}(c\to\Lambda_c)\times\mathcal{B}(\overline{c}\to eX)\times\mathcal{B}(\Lambda_c\to\Lambda X)\times[\epsilon(\Lambda_c\to\Lambda X)(\overline{c}\to eX)]}.$$

Note that the efficiency in the numerator of this equation refers to the correlated efficiency of having both the Λ and the electron in $\Lambda_c\to\Lambda e^+\nu_e$ pass all our selection criteria $[\epsilon(\Lambda_c\to\Lambda e\nu_e)=0.023\pm0.002]$; the efficiency in the denominator refers to the efficiency for having a Λ from a Λ_c decay pass our selection criteria in one hemisphere and also an electron from a generic charm decay pass our selection requirements in the opposite hemisphere $[\epsilon(\Lambda_c\to\Lambda X)(\overline{c}\to eX)=0.043\pm0.002]$. The efficiency is lower in the numerator due to the presence of momentum correlations between the Λ and the electron, resulting in a reduced efficiency for both particles to simultaneously pass the minimum momentum requirement $p>1$ GeV/c. The value for $\mathcal{B}(\overline{c}\to eX)$ (0.091 ± 0.008) is taken from data at $\sqrt{s}=10$ GeV [5]. Using the current Particle Data Group [5] value for $\mathcal{B}(\Lambda_c\to\Lambda e\nu_e)=0.021\pm0.006$ and our measured values for $N_{SH\text{-}SS}$ (445 ± 26) and $N_{OH\text{-}OS}$ (743 ± 32), we obtain an inferred value of $\mathcal{B}(\Lambda_c\to\Lambda X)\sim0.23\pm0.07$, where the error is statistical only. This is consistent with our measured product branching fraction for $\mathcal{B}_\Lambda=\mathcal{B}(c\to\Theta_c)\times\mathcal{B}(\Theta_c\to\Lambda X)$ if $\mathcal{B}(c\to\Theta_c)=6.67\%$, and assuming that $\mathcal{B}(c\to\Lambda_c)/\mathcal{B}(c\to\Theta_c)\approx1.0$.

VIII. SYSTEMATIC ERRORS

In order to determine additional systematic errors, we varied each of our individual particle and event requirements and noted the corresponding variation in our derived values for $\mathcal{B}(c\to\Theta_c)\times\mathcal{B}(\Theta_c\to\Lambda X)$. Typical variations were of order $\sim20\%$. Using this approach, we summarize our systematic dependencies in Table IV. The default values of, e.g., our kinematic cuts are defined, as well as the variation used to assess systematic dependences. For the pion and the electron tags, our largest systematic errors are due to uncertainties in the Monte Carlo event generation modeling, as determined using the ''wrong-sign'' yields. For the $\overline{D}$ tags, among the largest errors are the errors associated with signal extraction—this is assessed by determining the difference in the calculated final result when the signal and sideband regions are varied from their default values by $\pm30\%$. Realizing that (a) the $\overline{D}$ tags are consistently higher than the single-

track tags and (b) possible correlations in fragmentation between the two hemispheres have not been evaluated (nor are they present in our Monte Carlo simulations), we also take the rms spread in the values for $\mathcal{B}_\Lambda$ obtained with the four tags (14%) as an additional systematic error (added to each of the four individual measurements quoted below), reflecting the differences in the lepton-tagged vs π^-_{soft}-tagged vs D-tagged samples. Given the fact that the individual measurements are all consistent within errors, this is an admittedly very conservative approach.

IX. SUMMARY AND DISCUSSION

Using four different $e^+e^-\to c\bar{c}$ tags, and scaling our raw values by the D^0 cross-check as described above, we measure the product branching fraction $\mathcal{B}_\Lambda=\mathcal{B}(c\to\Theta_c X)\times\mathcal{B}(\Theta_c\to\Lambda X)$:

$$(1.68\pm0.10\pm0.40)\% \quad \text{(electron tags)}$$

$$(1.57\pm0.06\pm0.38)\% \quad \text{(soft pion tags)}$$

$$(2.09\pm0.08\pm0.41)\% \quad (\bar{D}^0 \text{ tags})$$

$$(1.95\pm0.13\pm0.47)\% \quad (D^- \text{ tags});$$

these results sum over the charmed baryons Θ_c produced at $\sqrt{s}=10$ GeV. Separating common from independent systematic errors, and weighting each result by the quadrature sum of its statistical error plus independent systematic error, we combine these four numbers to obtain a weighted product branching fraction:

$$\mathcal{B}_\Lambda=(1.87\pm0.03\pm0.33)\%.$$

In obtaining this result, we have not corrected for the statistical overlap between the four tag samples. Correcting for this would tend to slightly reduce the overall quoted statistical error. We can convert this result into a contour in the plane: $\mathcal{B}(\Theta_c\to\Lambda X)$ vs $\mathcal{B}(c\to\Theta_c)$, as shown in Fig. 7. Using the Monte Carlo value for $\mathcal{B}(c\to\Theta_c X)$ of 6.67% [this is consistent with the tabulated product cross-section $(e^+e^-\to c\bar{c})\times\mathcal{B}(c\to\Lambda_c)\cdot\mathcal{B}(\Lambda_c\to pK^-\pi^+)$ using $\mathcal{B}(\Lambda_c\to pK^-\pi^+)=5.0\%$], and taking the results from our four tags, we can infer a weighted average value:

$$\mathcal{B}(\Theta_c\to\Lambda X)=(28\pm1\pm5)\%.$$

It is important to note that this measurement is independent of the $\Lambda_c\to pK^-\pi^+$ normalization but is dependent on the Monte Carlo estimated value for $\mathcal{B}(c\to\Theta_c)$. This measurement is the first of its kind at $\sqrt{s}=10$ GeV.

In the simplest picture, a charmed baryon such as a Λ_c decays weakly through external W emission. Neglecting fragmentation at the lower vertex, this produces either a Σ^0 or, if isospin does not change, a Λ. Since all Σ^0's decay into Λ, we therefore expect that $\Lambda_c\to\Lambda X\approx100\%$ if the external spectator diagram dominates. This simple minded prediction

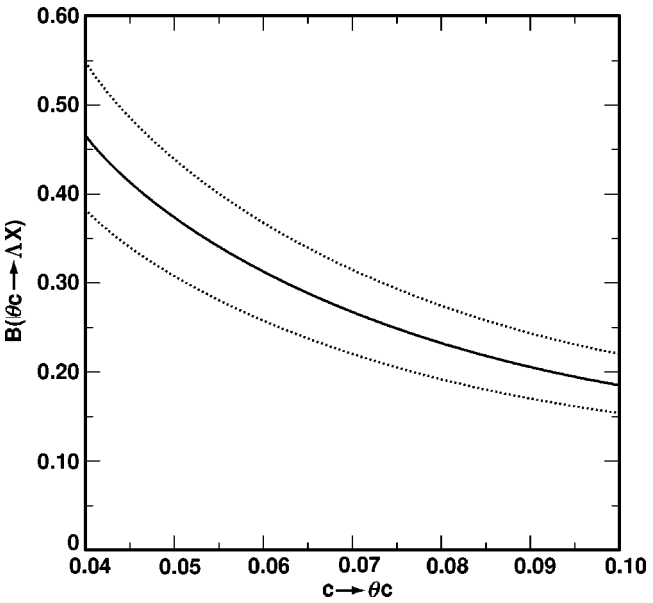

FIG. 7. Contour of $\mathcal{B}(\Theta_c\to\Lambda X)$ vs $c\to\Theta_c$ implied by our result. Contours corresponding to $\pm1\sigma$ excursions from our central value are also shown (dotted line). The Monte Carlo value for B_Λ $[\mathcal{B}(c\to\Theta_c)\times\mathcal{B}(\Theta_c\to\Lambda X)]$ is 0.0246, and the Monte Carlo expectation for $c\to\Theta_c$ is 0.0667.

is expected to be obeyed in semileptonic decays; i.e., $\mathcal{B}(\Lambda_c\to\Lambda l\nu)/\mathcal{B}(\Lambda_c\to Xl\nu)\to1$. Present data, however, give a value of approximately 50% for this ratio, albeit with large errors [5].

External and internal W emission, as well as W exchange can lead to NKX final states containing a nucleon and a K meson ($\Lambda_c\to pK^0_s$, e.g.). The fact that the Λ_c lifetime is only half that of the D^0 meson suggests that internal W-emission and W-exchange processes may comprise a large fraction of the total Λ_c width. Although internal W emission may be suppressed in decays of charmed mesons due to the color-matching requirement [which would predict $\mathcal{B}(D\to W_{int}X)/\mathcal{B}(D\to W_{ext}X)=1/9$], the larger number of degrees of freedom in baryon decays may mitigate this suppression, leading to a potentially large fraction of pKX final states. In the case of the Λ_c, W-exchange decays can produce either Λ's or NK in the final state, depending on the quark configuration. The naive expectation that the absence of exchange diagrams in Ξ_c^+ decays will lead to a longer lifetime for Ξ_c^+ compared to Ξ_c^0 and Λ_c is consistent with current experimental data.

The current world average for $\mathcal{B}(\Lambda_c\to\Lambda X)$ $(35\pm11)\%$ [5] is consistent with the notion that the simple minded external W-emission picture does not saturate Λ_c decays. The value for $\mathcal{B}(\Lambda_c\to\Lambda X)$ therefore has implications for the external versus internal spectator fractions in charmed baryon decay. Our results are therefore qualitatively consistent with a possibly substantial internal spectator contribution to charmed baryon decay.

Exclusive $\Lambda_c\to\Lambda X$ channels have also been measured; normalized to an estimate of $\mathcal{B}(\Lambda_c\to pK^-\pi^+)=(5.0\pm1.3)\%$ [5,16], the sum of the observed exclusive modes accounts for the bulk of the presently tabulated inclusive

$\Lambda_c \to \Lambda X$ rate $[\Sigma \mathcal{B}(\Lambda_c \to \Lambda + X)_{exclusive} / \mathcal{B}(\Lambda_c \to pK^- \pi^+) \sim 5$, where the sum includes a contribution of $\Sigma \mathcal{B}(\Lambda_c \to \Sigma^0 + X)_{exclusive} / \mathcal{B}(\Lambda_c \to pK^- \pi^+) \sim 1.5]$. We note that the difference between our inferred value for $\mathcal{B}(\Theta_c \to \Lambda X)$ and the sum of the exclusive Λ_c modes to Λ's [5] implies that most of the inclusive $\Lambda_c \to \Lambda X$ rate has been accounted for.

If charmed baryons produced in e^+e^- events are predominantly Λ_c's and if the JETSET expectation for $f(c \to \Lambda_c)$ is accurate, then our results are in agreement with the current world average for $\mathcal{B}(\Lambda_c \to \Lambda X)$. We note that the methodology of this analysis differs substantially from the previous CLEO analysis [4], which relied on a model of charmed baryon production in B decay to derive $\mathcal{B}(\Lambda_c \to \Lambda X)$.

Naively, one might expect fragmentation and decay of charmed baryons to be similar to bottom baryons. Using vertex tagging techniques, the OPAL Collaboration has determined $\mathcal{B}(b \to \Theta_b)\mathcal{B}(\Theta_b \to \Lambda X) = (3.50 \pm 0.32 \pm 0.35)\%$ [15]. Perhaps the simplest way to reconcile the two numbers is to assume (*ad hoc*) that $\mathcal{B}(b \to \Theta_b)$ at $\sqrt{s} \sim 90$ GeV is approximately twice as large as $\mathcal{B}(c \to \Theta_c)$ at $\sqrt{s} = 10$ GeV and that $\mathcal{B}(\Lambda_b \to \Lambda_c X) \approx 1.0$. However, the fact that the Λ_b lifetime is only 2/3 that of the B mesons [5] coupled with the fact that Λ_b has already been observed through $\Lambda_b \to \psi\Lambda$ implies that $\mathcal{B}(\Lambda_b \to \Lambda_c X) < 1$.

Finally, we stress that our final central value for $\mathcal{B}_\Lambda$ averages over the specific mix of charm tags that we use in this analysis. The composition of our $\bar{D}$-meson tags will not be the same as the composition of our electron tags, insofar as the lepton-tagged sample represents a weighted sum of $\bar{\Theta}_c \to l^- X$, $D_s^- \to l^- X$, $\bar{D}^0 \to l^- X$ and $D^- \to l^- X$. Our quoted final result can be general only if the two hemispheres in an $e^+e^- \to c\bar{c}$ event fragment independently. Although not yet measured, it is possible that there may be correlated $\bar{\Theta}_c \Theta_c$ production, in which case the likelihood of observing $\Theta_c \to \Lambda X$ would be larger for $\bar{\Theta}_c$ tags than for $\bar{D}$ tags, and the assumption of independent fragmentation would be invalid. A study of correlated $\bar{\Theta}_c \Theta_c$ production, presently in progress, will be the subject of a forthcoming publication.

ACKNOWLEDGMENTS

We gratefully acknowledge the effort of the CESR staff in providing us with excellent luminosity and running conditions. J.R. Patterson and I.P.J. Shipsey thank the NYI program of the NSF, M. Selen thanks the PFF program of the NSF, M. Selen and H. Yamamoto thank the OJI program of DOE, J.R. Patterson, K. Honscheid, M. Selen and V. Sharma thank the A.P. Sloan Foundation, M. Selen and V. Sharma thank the Research Corporation, F. Blanc thanks the Swiss National Science Foundation, and H. Schwarthoff and E. von Toerne thank the Alexander von Humboldt Stiftung for support. This work was supported by the National Science Foundation, the U.S. Department of Energy, and the Natural Sciences and Engineering Research Council of Canada.

[1] S. J. Sjostrand, computer code LUND 7.3, CERN Report No. CERN-TH-6488-92, 1992.
[2] K. Abe *et al.*, Phys. Rev. D **33**, 1 (1986).
[3] A. Adamovich *et al.*, Europhys. Lett. **4**, 887 (1987).
[4] CLEO Collaboration, G. Crawford *et al.*, Phys. Rev. D **45**, 752 (1992).
[5] Particle Data Group, C. Caso *et al.*, Eur. Phys. J. C **3**, 1 (1998).
[6] CLEO Collaboration, R. Ammar *et al.*, Phys. Rev. D **55**, 13 (1997).
[7] CLEO Collaboration, Y. Kubota *et al.*, Nucl. Instrum. Methods Phys. Res. A **320**, 66 (1992).
[8] G. Fox and S. Wolfram, Phys. Rev. Lett. **41**, 1581 (1978).
[9] G. Crawford *et al.*, Nucl. Instrum. Methods Phys. Res. A **345**, 429 (1994).
[10] CLEO Collaboration, M. Selen *et al.*, Phys. Rev. Lett. **71**, 1973 (1993).
[11] T. Hill *et al.*, Nucl. Instrum. Methods Phys. Res. A **418**, 32 (1998).
[12] CLEO Collaboration, R. Godang *et al.*, Phys. Rev. Lett. **84**, 5038 (2000).
[13] S. Jadach, Z. Was, R. Decker, and J. H. Kühn, Report No. CERN-TH.6793/93.
[14] ALEPH Collaboration, R. Barate *et al.*, Report No. CERN/EP 99-094, hep-ex/9909032.
[15] OPAL Collaboration, G. Abbiendi *et al.*, Eur. Phys. J. C **9**, 1 (1999).
[16] CLEO Collaboration, D. E. Jaffe *et al.*, Phys. Rev. D **62**, 072005 (2000).